International Journal of Research (IJR)
e-ISSN: 2348-6848
p-ISSN: 2348-795X
Vol. 11 Issue 05
May 2024

Prescribed-Time Formation Bipartite Containment of Layered Multi-agent Systems

Kaiyin Huang, Tao Li*, Jialong Tian, Zijie Jiang

School of Electrical Engineering and Automation, Hubei Normal University, Huangshi 435002, China

E-MAIL: taohust2008@163.com

Abstract

This paper aims to address the problem of prescribed-time formation bipartite containment for two-layered MASs (multi-agent systems). In this system, the leader layer engages in a purely cooperative relationship, while the follower layer engages in both cooperation and competition. Moreover, there exists a restraining relationship between the leader layer and corresponding follower layer. By introducing a time-varying function, this paper presents a novel prescribed-time distributed control protocol. The protocol is designed to drive all the leaders to form a formation within a specified time, while the followers simultaneously converge into the convex hulls formed by the states as well as the sign-inverted states of the leaders. Using Lyapunov stability theory, linear matrix inequality, the paper obtains the sufficient conditions for MASs to converge in a specified time and the stability about control algorithm is discussed in detail. Finally, a numerical simulation example is performed to verify the effectiveness of the presented theory.

Key words

Layered MAS; Formation bipartite containment; Prescribed-Time; Signed digraphs

1. Introduction

In the last 20 years, multi-agent systems (MASs) have been studied by researchers given its broad applications, e.g. in security, spacecraft formation flying, search and rescue missions, among others [1-3]. The main research area of MASs is cooperative control, where the fundamental problems are consensus, formation and containment, collision avoidance, and the formation containment problem, among others.

As mentioned above, formation containment control is a important research problem of MASs. The formation containment problem consists of a subset of agents, called followers, remaining within a space formed by another subset of agents, called leaders. For instance, a cluster of self-driving vehicles transitioning towards a specified zone. Among them, certain leading vehicles come outfitted with sensors. Their objective lies in identifying potentially dangerous obstacles and arranging themselves into a preferred layout. Meanwhile, following vehicles must maintain their position within the boundary defined by the leading vehicles. Dong et al. [4] combined formation control with containment control methods, driving all the leaders to form a formation, while the followers converge into the convex hull formed by the states of the leaders. Works related to the formation containment problem of homogeneous systems can be found in [5,6]. On the other hand, some works addressing the formation containment problem with heterogeneous systems can be found in [7,8]. Formation containment control problems for second-order MASs were studied in [9,10]. In the reference [11], formation containment protocols for general linear MASs were presented. Formation containment control has significant applications in domains such as autonomous unmanned systems, logistics, and the military [12,13]. It enables agents to accomplish tasks efficiently, enhancing safety and reliability.

However, the aforementioned works does not discuss formation containment control under the framework of signed networks. In many real world scenarios such as social networks, trust networks, marketing or games, and biological systems, the relationships/interactions among individuals may be friendly/cooperative or hostile/antagonistic [14-18]. They can be represented as signed networks, which can be characterized by graphs that accommodate not just positive, but also negative adjacency weights. Studying MASs under signed networks is more practically meaningful.

***Received**: 12 April 2024*
***Revised**: 24 April 2024*
***Accepted:** 6 May 2024*

 DOI: https://doi.org/10.5281/zenodo.11123257

International Journal of Research (IJR)
e-ISSN: 2348-6848
p-ISSN: 2348-795X
Vol. 11 Issue 05
May 2024

Note that all the aforementioned works on formation containment control focus on analyses and applications of synchronization of single layer complex dynamical networks which may oversimplify some systems in the real world. In contrast to MASs with a single layer, the practical applications of layered MASs in real-world domains have garnered significant attention from researchers. The increased attention is caused by the potential advantages of layered MASs in modeling real-world networks, such as power grids and APP social networks. In aforementioned formation containment control studies, the follower be required to track the convex combination of all leaders' states, rather than the states of a particular leader. These mean that the follower's behavior and control inputs are influenced by the states of all leaders. However, this consideration of localized interactions between leaders and followers does not align with certain real-world scenarios. For example, in the multi-robot systems, the follower robot may need to closely follow a specific leader robot while disregarding the movements of other leader robots. Building upon these observations and the concept of consensus tracking. Wen et al.[15] introduced the notion of node-to-node consensus. Scholars have carried out theoretical research on MASs in two-layered networks [19,20]. In this framework, MASs are composed of two layers: a leader layer and a follower layer. Each layer consists of an equal number of agents, and during the evolution of the systems, certain agents in the follower layer are "pinned". The layered MASs can achieve the global objective of the networks by designing a local control strategy within each layer. This approach significantly reduces the complexity of the network model design. Therefore, it is meaningful to discuss the formation containment control problem of MASs in layered network.

In practical applications, convergence time is a crucial factor when determining system performance. Progressive convergence refers to the gradual tendency of the states of agents to approach a certain target state over time. It may require an infinite amount of time to fully reach the target, which implies that the convergence speed of the system can be slow and even unpredictable. Finite-time convergence occurs when the agents attain the target state within a finite duration. This convergence property is more desirable in certain applications as it guarantees that the convergence time of the system is bounded, but it is dependent on the initial conditions. Fixed-time convergence denotes the agents achieving the target state within a fixed-time period, regardless of the initial system state. However, while existing fixed-time control methods are affected by parameters, and sometimes these parameters are unknown. In the past few years, many fruitful results have been obtained concerning fixed-time formation or containment of MASs [21-24]. Moreover, whether it is finite-time convergence or fixed-time convergence, it cannot guarantee that the system converges to a desired state at specified time. Therefore, these methods cannot be applied to some applications that have a high requirement of control accuracy and convergence speed. For example, consider an earthquake or other emergency situation that requires the rapid coordination of multiple unmanned aerial vehicles (UAVs) for searching disaster-stricken areas or delivering supplies. In such a scenario, the collaborative efforts of the team need to achieve specific dynamic behaviors within a given timeframe to ensure the successful completion of the mission. To address this shortcoming, a prescribed-time method has been proposed by scholars. For instance, in the reference [25], a novel distributed control method for achieving consensus and containment in MASs within a prescribed time frame has been developed. However, research on formation-containment control at a prescribed time is limited.

The above observations inspire us to tackle the challenge of prescribed-time formation bipartite containment of two-layered MASs. This paper presents a novel prescribed-time distributed control method for formation bipartite containment of two-layered MASs in which not only the finite convergence time can be explicitly prespecified but also the control action is smooth everywhere. Ultimately, the leaders are capable of shaping a formation within the specified time, while the followers achieve convergence within the convex hulls formed by the states as well as the sign-inverted states of the leaders at the same time.

The rest parts of this paper have several sections, section 2 provides essential background information on graph theory and matrix theory, as well as the formulation of the model. The primary analytical findings are presented in Section 3. A numerical example illustrates the analytical results' effectiveness in Section 4 and Section 5 presents the conclusions.

2. Preliminaries and statement of problem

2.1. Graph theory

This paper investigates a type of MASs that is composed of two layers: a leader layer and a follower layer. Each layer contains n agents. The leaders exclusively receive information from other leaders, whereas the followers can receive information from both other followers and leaders.

Let $G_L = (V^L, \varepsilon^L, B)$ represent the communication topology of the leaders, which is a directed non-negative graph with n nodes. Here, $V^L = \{v_1^L, v_2^L, \cdots, v_n^L\}$ represents the node set, where the indices of nodes belong to $\varpi = \{1, 2, \cdots, n\}$; $\varepsilon^L = \{(j,i) : b_{ij} > 0\}$ represents the edge set, where b_{ij} denotes the weight of edge (j,i) ;

Received: 12 April 2024
Revised: 24 April 2024
Accepted: 6 May 2024

DOI: https://doi.org/10.5281/zenodo.11123257

$\mathrm{B}=[b_{ij}]\in \mathrm{R}^{n\times n}$ is the adjacency matrix, where $b_{ij}\geq 0$. The $\mathrm{G}_F=(\mathrm{V}^F,\varepsilon^F,\mathrm{A})$ represent the communication topology of the followers, which is a symbolic graph with n nodes, $\mathrm{V}^F=\{v_1^F,v_2^F,\cdots,v_n^F\}$ represents the node set, $\varepsilon^F=\{(j,i):a_{ij}\neq 0\}$ represents the edge set, where a_{ij} denotes the weight of edge (j,i). $\mathrm{A}=[a_{ij}]\in \mathrm{R}^{n\times n}$ is the adjacency matrix, where $a_{ij}>0$ indicates a positive connection (cooperation) between agent nodes i and j, $a_{ij}<0$ indicates a negative connection (competition) between agent nodes i and j, and $a_{ij}=0$ indicates no connection between agent nodes i and j. Let the Laplacian matrices of graphs G_L and G_F be denoted as $L_L=[l_{ij}^L]\in \mathrm{R}^{n\times n}$ and $L_F=[l_{ij}^F]\in \mathrm{R}^{n\times n}$, they are written as:

$$l_{ij}^L=\begin{cases}\sum_{k=1}^{n} b_{ik} & ,i=j\\ -b_{ik} & ,i\neq j\end{cases}\qquad ,\ l_{ij}^F=\begin{cases}\sum_{k=1}^{n}|a_{ik}| & ,i=j\\ -a_{ij} & ,i\neq j\,.\end{cases}$$

Let p_j represent the weight assigned to the pinning edges connecting the leader j and the follower j, $j=1,2,\cdots,n$. By relabeling the leader layer as a single agent 0, we can reconstruct a graph G which its Laplacian matrix can be expressed as follows:

$$\mathrm{L}=\begin{pmatrix}0 & 0_n^T\\ -\mathrm{P} & \Lambda\end{pmatrix},$$

where $\mathrm{P}=[p_1,\cdots,p_n]^T$, $\Lambda=L_F+p$, $p=diag\{p_1,\cdots,p_n\}$.

2.2. Some lemmas and definitions

Definition 1 Error! Reference source not found.: If there exists a set of subsets $\{\mathrm{V}_k^F\}$, $k=1,2,\cdots l$ in the node set V^F of the signed graph G_F that satisfies the conditions:
$\mathrm{V}^F=v_1^F\cup v_2^F\cup\cdots\cup v_l^F$ and $v_i^F\cup v_j^F=\varnothing(i\neq j;i,j\in k)$, then it is said that $v_1^F,v_2^F,\cdots,v_l^F$ form a partition of the set V^F.

Definition 2 Error! Reference source not found.: A signed graph G_F is said to be structurally balanced if it admits a bipartition of note v_1^F and v_2^F, satisfying $v_1^F\cup v_2^F=\mathrm{V}^F$ and $v_1^F\cap v_2^F=\varnothing$, such that $a_{ij}\geq 0$, $i,j\in \mathrm{V}_q^F\,(q\in\{1,2\})$ and $a_{ij}\leq 0$, $i\in \mathrm{V}_q^F$, $j\in \mathrm{V}_{3-q}^F$.

A time-varying function is proposed as follows

$$\mu(t)=\begin{cases}\dfrac{T^h}{(T+t_0-t)^h} & ,t\in[t_0,t_1)\\ 1, & ,t\in[t_1,\infty)\,,\end{cases}\tag{1}$$

where $t_1=t_0+T$, $h>2$ represents an arbitrary real number chosen by the user, and $T\geq T_s>0$ with T_s being the time period needed for signal processing/computing and information transmission/communication. Note that $\mu^{-q}(q>0)$ is monotonically decreasing on $[t_0,t_1)$, $\mu(t_0)^{-q}=1$ and $\lim_{t\to t_1^-}\mu(t)^{-q}=0$. In addition

$$\dot{\mu}(t)=\begin{cases}\dfrac{h}{T}\mu^{1+\frac{1}{h}} & ,t\in[t_0,t_1)\\ 0 & ,t\in[t_1,\infty)\,,\end{cases}\tag{2}$$

in this context, we utilize the right-hand derivative of $\mu(t)$ at $t=t_1$ as $\dot{\mu}(t_1)$.

Lemma 1 Error! Reference source not found.: Consider system $\dot{x}(t)=f(t,x(t))$, let $V(x(t),t):W\times R_+\to R$ be a continuously differentiable function and $W\subset R^m$ be a domain containing the origin. If there exists a real constant $b>0$ such that

$$V(0,t)=0 \text{ and } V(x(t),t)>0 \text{ in } W-\{0\}$$

$$\dot{V}=-bV-2\frac{\dot{\mu}}{\mu}V \text{ in } W$$

Received: *12 April 2024*
Revised: *24 April 2024*
Accepted: *6 May 2024*

DOI: https://doi.org/10.5281/zenodo.11123257

on $[t_0,\infty)$, then the origin of system is prescribed-time stable with the prescribed time T. If $W=R^m$, then the origin of system is globally prescribed-time stable with the prescribed time T. In addition, for $t\in[t_0,t_1)$, it holds that

$$V(t)\le \mu^{-2}\exp(-b(t-t_0))V(t_0),$$

and for $t\in[t_1,\infty)$, it holds that $V(t)\equiv 0$.

Lemma 2 [25]**:** There exists a positive diagonal matrix $Q=diag\{q_1,\ldots,q_n\}\in \mathbb{R}^{m\times m}$ such that

$$J=Q\Lambda+(\Lambda)^T Q>0.$$

In which $q_1,\ldots,q_n$ are chosen as $[q_1,\ldots,q_n]^T=(\Lambda)^{-T}1_n$.

2.3 Problem statement

We consider the whole $2n$ agents making up the two-layered MASs, the leader layer and the follower layer consist of n agents each, with the dynamics of the agents in the leader layer being characterized as follows:

$$\dot{x}_i(t)=u_{xi}(t),\ i=1,\ldots,n, \qquad (3)$$

where $x_i(t)\in\mathbb{R}^m$, $u_{xi}(t)\in\mathbb{R}^m$ denote the position and control input of the agents in the leader layer, respectively.

The dynamics of the *ith* follower is given by

$$\dot{y}_i(t)=u_{yi}(t),\ i=1,\ldots,n, \qquad (4)$$

where $y_i(t)\in\mathbb{R}^m$, $u_{yi}(t)\in\mathbb{R}^m$ denote the position and control input of the agents in the follower layer, respectively.

In this paper, we are interested in investigating prescribed-time formation bipartite containment problem of MASs, which is defined as follows.

Definition 3 [27]: If leaders can form a desired formation within a specified time T, while followers can enter the convex hulls formed by the states as well as the sign-inverted states of the leaders at the same time, then the MASs can realize prescribed-time formation bipartite containment control. In other words, both of the following conditions are satisfied.

1) For any given expected formation vector $h_i\in\mathbb{R}^m$, the leaders are said to achieve prescribed-time state formation if $\lim_{t\to T}\left\|x_i-h_i-(x_j-h_j)\right\|=0$ and $\left\|x_i-h_i-(x_j-h_j)\right\|=0,\forall t>T$.

2) For MASs (3) and (4), the bipartite containment is achieved if all followers' states $y(t)$ converge to the convex hulls formed by the leaders' state $x(t)$ and the reverse leaders' states $-x(t)$. That is to say, the following conditions hold:

$$\lim_{t\to T}\left\|y(t)-(\Lambda\otimes I_m)^{-1}(p\otimes I_m)x(t)\right\|=0 \text{ and } \left\|y(t)-(\Lambda\otimes I_m)^{-1}(p\otimes I_m)x(t)\right\|=0,\forall t>T.$$

The definitions of the formation errors and the bipartite containment errors are provided as follows:

$$e_{xi}=\sum_{j=1}^{n}a_{ij}[(x_i-h_i)-(x_j-h_j)]. \qquad (5)$$

$$e_{yi}=\sum_{j=1}^{n}a_{ij}(sign(a_{ij})y_i-y_j)+p_i(sign(p_i)y_i-x_i). \qquad (6)$$

Let $e_y=[e_{y1}^T,\ldots,e_{yn}^T]^T$, $p=diag\{p_1,\ldots,p_n\}$, $P=diag\{|p_1|,\ldots,|p_n|\}$. Then it holds

$$\begin{aligned}e_y(t)&=(L\otimes I_m)y(t)+(P\otimes I_m)y(t)-(p\otimes I_m)x(t)\\&=((L+P)\otimes I_m)y(t)-(p\otimes I_m)x(t)\\&=(\Lambda\otimes I_m)y(t)-(p\otimes I_m)x(t)\\&=(\Lambda\otimes I_m)(y(t)-(\Lambda\otimes I_m)^{-1}(p\otimes I_m)x(t)).\end{aligned} \qquad (11)$$

3. Control protocol design and stability analysis

In this section, two control inputs will be independently raised in order to achieve the prescribed-time formation bipartite containment.

Having completed the aforementioned preparation, we are now able to introduce the prescribed-time formation bipartite containment control protocol. The control protocols for leaders and followers are designed separately:

Received*: 12 April 2024*
Revised*: 24 April 2024*
Accepted: *6 May 2024*

DOI: https://doi.org/10.5281/zenodo.11123257

$$u_{xi} = -(d_x + c_x \frac{\dot{\mu}}{\mu}) e_{xi}, \; i = 1, \ldots, n \tag{7}$$

$$u_{yi} = -(d + c\frac{\dot{\mu}}{\mu}) e_{yi} + ((\Lambda)^{-1} p \otimes I_m)_i (-(d_x + c_x \frac{\dot{\mu}}{\mu})) e_{xi}, \; i = 1, \ldots, n, \tag{8}$$

where $d, d_x > 0$ and $c, c_x > 0$ are design parameters. They can be expressed in the following concise format:

$$u_x = -(d_x + c_x \frac{\dot{\mu}}{\mu}) e_x \tag{9}$$

$$u_y = -(d + c\frac{\dot{\mu}}{\mu}) e_y + ((\Lambda)^{-1} p \otimes I_m)(-(d_x + c_x \frac{\dot{\mu}}{\mu}) e_x), \tag{10}$$

where $u_y = [u_{y1}^T, \ldots u_{yn}^T]^T \in R^{m\times n}$, $u_x = [u_{x1}^T, \ldots u_{xn}^T]^T \in R^{m\times n}$.

According to Definition1, the prescribed-time formation bipartite containment objective is achieved if $e_x(t)$ and $e_y(t)$ converges to zero within the specified finite time T. We are now prepared to present the following result.

Theorem 1: Consider system (3) and (4) under the control protocol (9) and (10) with $d_x \ge [(1/(\lambda_2(\mathcal{L}))]$ and $d \ge [(2\lambda_{\max}(Q))/(\lambda_1(J))]$, solved the prescribed-time formation bipartite containment problem within the prespecified finite time T in that

$$\|e_x(t)\| \le \mu^{-1} \exp(-d_x \lambda_2(\mathcal{L})(t - t_0)) \|e_x(t_0)\|, \tag{12}$$

$$\|e_y(t)\| \le \mu^{-1} \exp(-\frac{d\lambda_1(J)}{2\lambda_{\max}(Q)}(t - t_0)) \times \sqrt{\frac{\lambda_{\max}(Q)}{\lambda_{\min}(Q)}} \|(\Lambda \otimes I_m)^{-1}\| \cdot \|e(t_0)\|,$$

for all $t \in [t_0, t_1)$. Furthermore, u_x and u_y remain constant at zero throughout $[t_1, \infty)$, and the control input signals remain C^1 smooth and uniformly bounded over the whole time interval $[t_0, \infty)$.

Proof: The proof is divided into the following six steps.

Step1: The formation is achieved within T and u_x is smooth and uniformly bounded on $[t_0, t_1)$.

By selecting the Lyapunov function candidate as

$$V_x = \frac{1}{2} e_x^T(t) e_x(t). \tag{13}$$

According to (5), we have

$$\begin{aligned} \dot{e}_x(t) &= (\mathcal{L} \otimes I_m)\dot{x}(t) \\ &= (\mathcal{L} \otimes I_m)(-(d_x + c_x \frac{\dot{\mu}}{\mu}) e_x). \end{aligned} \tag{14}$$

Taking the derivative of V_x gives

$$\begin{aligned} \dot{V}_x &= e_x^T \dot{e}_x \\ &= e_x^T [(\mathcal{L} \otimes I_m)(-(d_x + c_x \frac{\dot{\mu}}{\mu}) e_x)] \\ &= e_x^T [-(d_x + c_x \frac{\dot{\mu}}{\mu})(\mathcal{L} \otimes I_m)] e_x \\ &= -d_x e_x^T (\mathcal{L} \otimes I_m) e_x - c_x \frac{\dot{\mu}}{\mu} e_x^T (\mathcal{L} \otimes I_m) e_x \\ &\le -d_x \lambda_2(\mathcal{L}) e_x^T e_x - c_x \frac{\dot{\mu}}{\mu} \lambda_2(\mathcal{L}) e_x^T e_x \\ &\le -2 d_x \lambda_2(\mathcal{L}) V_x - 2\frac{\dot{\mu}}{\mu} V_x. \end{aligned} \tag{15}$$

According to lemma1, we have from (15) that

$$\|e_x(t)\|^2 \le \mu^{-2} \exp(-2 d_x \lambda_2(\mathcal{L})(t - t_0)) \|e_x(t_0)\|^2 \tag{16}$$

Received: *12 April 2024*
Revised: *24 April 2024*
Accepted: *6 May 2024*

DOI: https://doi.org/10.5281/zenodo.11123257

on $[t_0,t_1)$, which yields (12), and by utilizing the fact that $\mu^{-1}\to 0$ as $t\to t_1^-$. $\|e_x(t)\|\to 0$ as $t\to t_1^-$. It can be observed that the formation is accomplished within the predetermined time frame of T.

By recalling that $0<\mu^{-1}\le 1$, $0<\mu^{\frac{1}{h}-1}\le 1$ and $0<\exp(-d_x\lambda_2(\mathrm{L})(t-t_0))\le 1$, we have

$$\|e_x(t)\|\le \mu^{-1}\exp(-d_x\lambda_2(\mathrm{L})(t-t_0))\|e(t_0)\|\in L_\infty \tag{17}$$

$$\left\|\frac{\dot\mu}{\mu}e_x\right\|\le \frac{h}{T}\mu^{\frac{1}{h}-1}\exp(-d_x\lambda_2(\mathrm{L})(t-t_0))\|e(t_0)\|\in L_\infty, \tag{18}$$

both of which result in

$$\begin{aligned}\|u_x\|&\le d_x\|e_x\|+c_x\left\|\frac{\dot\mu}{\mu}e_x\right\|\\ &\le d_x\mu^{-1}\exp(-d_x\lambda_2(\mathrm{L})(t-t_0))\|e(t_0)\|\\ &+c_x\frac{h}{T}\mu^{\frac{1}{h}-1}\exp(-d_x\lambda_2(\mathrm{L})(t-t_0))\|e(t_0)\|\\ &\le (d_x+c_x\frac{h}{T})\|e(t_0)\|\in L_\infty\end{aligned} \tag{19}$$

on $[t_0,t_1)$. From (19), it is evident that the control input is uniformly bounded on $[t_0,t_1)$.

By examining $\dot u_x$ on $[t_0,t_1)$, we get

$$\begin{aligned}\dot u_x&=-(d_x+c_x\frac{h}{T}\mu^{\frac{1}{h}})\dot e_x-c_x\frac{h}{T}\frac{1}{h}\mu^{\frac{1}{h}-1}\dot\mu e_x\\ &=(d_x+c_x\frac{h}{T}\mu^{\frac{1}{h}})(\mathrm{L}\otimes I_m)(d_x+c_x\frac{h}{T}\mu^{\frac{1}{h}})e_x-c_x\frac{h}{T}\frac{1}{h}\frac{h}{T}\mu^{\frac{2}{h}}e_x\\ &=(d_x^2+2d_xc_x\frac{h}{T}\mu^{\frac{1}{h}}+c_x^2(\frac{h}{T})^2\mu^{\frac{2}{h}})(\mathrm{L}\otimes I_m)e_x-c_x\frac{h}{T}\frac{1}{h}\frac{h}{T}\mu^{\frac{2}{h}}e_x,\end{aligned} \tag{20}$$

from which we see that both u_x and $\dot u_x$ are continuous with respect to t on $[t_0,t_1)$, and therefore u_x is C^1 smooth with respect to t on $[t_0,t_1)$.

Step 2: The formation is maintained and the control input u_x remains constant at zero throughout $[t_1,\infty)$. We readily obtain

$$\dot V_x\le -d_x\lambda_2\mathrm{L}V_x,\ t\in[t_1,\infty), \tag{21}$$

by recognizing $e_x(t)$ is continuous at $t=t_1$. Consequently, we have $V_x(t)$ is continuous at $t=t_1$, and therefore,

$$V_x(t_1)=\lim_{t\to t_1^-}\frac{1}{2}e_x^T(t)e_x(t)=0. \tag{22}$$

combining (21) and (22) yields

$$0\le V_x(t)\le V_x(t_1)=0. \tag{23}$$

That is $V_x(t)\equiv 0$ on $t\in[t_1,\infty)$. Thus $e_x(t)\equiv 0_{mn}$. From the definition of u_x, we deduce that $u_x\equiv 0_{mn}$ on $[t_1,\infty)$. Taken together, these findings demonstrate that the formation is preserved, and the control input remains at zero throughout the duration of $[t_1,\infty)$ using the provided control law.

Step 3: Now we simply need to confirm that u_x and $\dot u_x$ exist and are continuous with respect to t at $t=t_1$.

It is clear that $\lim_{t\to t_1^-}u_x=0_{mn}$ from the second inequality in (19) and $\lim_{t\to t_1^+}u_x=0_{mn}=u_x(t_1)$, implying that u_x exists and is continuous at $t=t_1$. Now we investigate each term of $\dot u_x$ on the right hand of (20) to establish its existence and continuity at $t=t_1$. By utilizing the fact that $\mu^{\frac{1}{h}-1}\to 0$, $\mu^{\frac{2}{h}-1}\to 0$ as $t\to t_1^-$, and $\|\mu e_x\|\in L_\infty$ on $[t_0,t_1)$ guaranteed by (16), it is obvious that

$$\|(\mathrm{L}\otimes I_m)e_x\|\to 0 \tag{24}$$

$$\left\|\mu^{\frac{1}{h}}(\mathrm{L}\otimes I_m)e_x\right\|\le \mu^{\frac{1}{h}-1}\|(\mathrm{L}\otimes I_m)\|\|\mu e_x\|\to 0 \tag{25}$$

Received: 12 April 2024
Revised: 24 April 2024
Accepted: 6 May 2024

DOI: https://doi.org/10.5281/zenodo.11123257

$$\left\| \mu^{\frac{2}{h}} (\mathrm{L} \otimes I_m) e_x \right\| \le \mu^{\frac{2}{h}-1} \|(\mathrm{L} \otimes I_m)\| \|\mu e_x\| \to 0 \qquad (26)$$

$$\left\| \mu^{\frac{2}{h}} e_x \right\| \le \mu^{\frac{2}{h}-1} \|\mu e_x\| \to 0 , \qquad (27)$$

as $t \to t_1^-$. By inserting (24)-(27) into (20), we obtain $\|\dot{u}_x\| \to 0$ as $t \to t_1^-$. Then we have

$$\lim_{t \to t_1^-} \|\dot{u}_x\| = 0 = \lim_{t \to t_1^+} \|\dot{u}_x\| \qquad (28)$$

and therefore,

$$\lim_{t \to t_1^-} u_x = 0_{mn} = \lim_{t \to t_1^+} u_x . \qquad (29)$$

This implies that $\dot{u}_x$ exists and is continuous at $t = t_1$. By observing that both u_x and $\dot{u}_x$ exists and are continuous at $t = t_1$, based on the definitions of continuity and smoothness, we can therefore deduce that u_x is C^1 smooth with respect to t at $t = t_1$, and thus u_x is C^1 smooth with respect to t on $[t_0, \infty)$.

Step4: The bipartite containment is achieved within T and the control input u_y is C^1 smooth and uniformly bounded on $[t_0, t_1)$.

Choosing the Lyapunov function candidate as

$$V_y = e_y^T(t)(Q \otimes I_m) e_y(t) , \qquad (31)$$

according to (11), we have

$$\begin{aligned} \dot{e}_y(t) &= (\Lambda \otimes I_m)(\dot{y}(t) - (\Lambda \otimes I_m)^{-1}(p \otimes I_m)\dot{x}(t)) \\ &= (\Lambda \otimes I_m)(-(d + c\frac{\dot{\mu}}{\mu})e_y) . \end{aligned} \qquad (32)$$

We derive from lemma2 and (32) that

$$\begin{aligned} \dot{V}_y &= 2e_y^T(t)(Q \otimes I_m)\dot{e}_y(t) \\ &= 2e_y^T(t)(Q \otimes I_m)(\Lambda \otimes I_m)(-(d + c\frac{\dot{\mu}}{\mu})e_y) \\ &= -(d + c\frac{\dot{\mu}}{\mu})e_y^T(t)[(Q\Lambda + (\Lambda)^T Q) \otimes I_m]e_y \\ &= -(d + c\frac{\dot{\mu}}{\mu})e_y^T(t)(J \otimes I_m)e_y(t) \\ &\le -d\lambda_1(J)e_y^T(t)e_y - c\frac{\dot{\mu}}{\mu}\lambda_1(J)e_y^T(t)e_y(t) \\ &\le -d\frac{\lambda_1(J)}{\lambda_{\max}(Q)}V_y - c\frac{\dot{\mu}}{\mu}\frac{\lambda_1(J)}{\lambda_{\max}(Q)}V_y \\ &\le -d\frac{\lambda_1(J)}{\lambda_{\max}(Q)}V_y - 2\frac{\dot{\mu}}{\mu}V_y . \end{aligned} \qquad (33)$$

According to lemma1, we get from (33) that

$$V_y \le \mu^{-2} \exp(-d\frac{\lambda_1(J)}{\lambda_{\max}(QJ)}(t - t_0))V_y(t_0) , \qquad (34)$$

this implies

$$\|e_y(t)\|^2 \le \mu^{-2} \exp(-d\frac{\lambda_1(J)}{\lambda_{\max}(Q)}(t - t_0)) \times \frac{\lambda_{\min}(Q)}{\lambda_{\max}(Q)}\|e_y(t_0)\|^2 , \qquad (35)$$

and then

$$\begin{aligned} &\|y(t) - (\Lambda \otimes I_m)^{-1}(p \otimes I_m)x(t)\| \\ &= \|(\Lambda \otimes I_m)^{-1}e_y(t)\| \le \|(\Lambda \otimes I_m)^{-1}\|\|e_y(t)\| \\ &\le \mu^{-1} \exp(-d\frac{\lambda_1(J)}{2\lambda_{\max}(Q)}(t - t_0)) \end{aligned}$$

Received: 12 April 2024
Revised: 24 April 2024
Accepted: 6 May 2024

DOI: https://doi.org/10.5281/zenodo.11123257

$$\times\sqrt{\frac{\lambda_{\min}(Q)}{\lambda_{\max}(Q)}}\left\|(\Lambda\otimes I_m)^{-1}\right\|\left\|e_y(t_0)\right\|, \qquad (36)$$

which yield (30). From (36) we get

$$\left\|y(t)-(\Lambda\otimes I_m)^{-1}(p\otimes I_m)x(t)\right\|\to 0 \text{ as } t\to t_1^-, \qquad (37)$$

that is, $y(t)\to(\Lambda\otimes I_m)^{-1}(p\otimes I_m)x(t)$ as $t\to t_1^-$, bipartite containment is accomplished within the specified finite time T.

Note that $L_\infty := \{z(t)\,|\,z:\mathrm{R}_+\to\mathrm{R}, \sup_{t\in\mathrm{R}_+}|z(t)|<\infty\}$, By recalling that $0<\mu^{-1}\le 1, 0<\mu^{1/h-1}\le 1, 0<\exp(-\frac{d\lambda_1(J)}{2\lambda_{\max}(Q)}(t-t_0))\le 1$, we then have

$$\begin{aligned}\left\|e_y(t)\right\| &\le \mu^{-1}\exp(-\frac{d\lambda_1(J)}{2\lambda_{\max}(Q)}(t-t_0)\times\sqrt{\frac{\lambda_{\max}(Q)}{\lambda_{\min}(Q)}}\left\|(\Lambda\otimes I_m)^{-1}\right\|\cdot\left\|e_y(t_0)\right\| \\ &\le m\sqrt{\frac{\lambda_{\max}(Q)}{\lambda_{\min}(Q)}}\left\|(\Lambda)^{-1}\right\|\cdot\left\|e_y(t_0)\right\|\in L_\infty .\end{aligned} \qquad (38)$$

$$\begin{aligned}\left\|\frac{\dot{\mu}}{\mu}e_y\right\| &= \frac{h}{T}\mu^{1/h}\left\|e_y(t)\right\| \\ &\le \frac{h}{T}m\mu^{1/h-1}\exp(-\frac{d\lambda_1(J)}{2\lambda_{\max}(Q)}(t-t_0)) \\ &\times\sqrt{\frac{\lambda_{\max}(Q)}{\lambda_{\min}(Q)}}\left\|(\Lambda)^{-1}\right\|\cdot\left\|e_y(t_0)\right\| \\ &\le \frac{h}{T}m\sqrt{\frac{\lambda_{\max}(Q)}{\lambda_{\min}(Q)}}\left\|(\Lambda)^{-1}\right\|\cdot\left\|e_y(t_0)\right\|\in L_\infty ,\end{aligned} \qquad (39)$$

both of which yield

$$\begin{aligned}\left\|u_y\right\| &\le d\left\|e_y(t)\right\| + c\frac{h}{T}\left\|\frac{\dot{\mu}}{\mu}e_y\right\| \\ &+\left\|((\Lambda)^{-1}p\otimes I_m)(-(d_x+c_x\frac{\dot{\mu}}{\mu})e_x\right\|\in L_\infty\end{aligned} \qquad (40)$$

on $[t_0,t_1)$. From (40), it is evident that the control input is uniformly bounded on $[t_0,t_1)$.

By analyzing u_y and $\dot{u}_y$ from (5), on $[t_0,t_1)$, we get

$$\begin{aligned}u_y &= -(d+c\frac{\dot{\mu}}{\mu})(\Lambda\otimes I_m)(y(t)-((\Lambda)^{-1}p\otimes I_m)x(t)) \\ &+((\Lambda)^{-1}p\otimes I_m)(-(d_x+c_x\frac{\dot{\mu}}{\mu})e_x) .\end{aligned} \qquad (41)$$

$$\begin{aligned}\dot{u}_y &= -(d+c\frac{h}{T}\mu^{1/h})\dot{e}_y(t) - c\frac{h}{T}\frac{1}{h}\mu^{1/h-1}\dot{\mu}e_y(t) \\ &+((\Lambda)^{-1}p\otimes I_m)[(-(d_x+c_x\frac{h}{T}\mu^{1/h})(\mathrm{L}\otimes I_m) \\ &\times(-(d_x+c_x\frac{h}{T}\mu^{1/h})e_x - c_x\frac{h}{T}\frac{1}{T}\mu^{2/h}e_x)] \\ &= -(d+c\frac{h}{T}\mu^{1/h})(\Lambda\otimes I_m)(-(d+c\frac{\dot{\mu}}{\mu})e_y) - c\frac{h}{T}\frac{1}{h}\mu^{1/h-1}\dot{\mu}e_y(t) \\ &+((\Lambda)^{-1}p\otimes I_m)[(-(d_x+c_x\frac{h}{T}\mu^{1/h})(\mathrm{L}\otimes I_m) \\ &\times(-(d_x+c_x\frac{h}{T}\mu^{1/h})e_x - c_x\frac{h}{T}\frac{1}{T}\mu^{2/h}e_x)]\end{aligned}$$

Received: 12 April 2024
Revised: 24 April 2024
Accepted: 6 May 2024

DOI: https://doi.org/10.5281/zenodo.11123257

e-ISSN: 2348-6848
p-ISSN: 2348-795X
Vol. 11 Issue 05
May 2024

$$
\begin{aligned}
&= -(d + c\frac{h}{T}\mu^{1/h})(-(d + c\frac{h}{T}\mu^{1/h})(\Lambda \otimes I_m)(\Lambda \otimes I_m) \\
&\times (y(t) - ((\Lambda)^{-1} p \otimes I_m)x(t))) - c\frac{h}{T}\frac{1}{T}\mu^{2/h}(\Lambda \otimes I_m) \\
&\times (y(t) - (\Lambda \otimes I_m)^{-1}(p \otimes I_m)x(t)) \\
&+ ((\Lambda)^{-1} p \otimes I_m)[(-(d_x + c_x\frac{h}{T}\mu^{1/h})(\mathrm{L} \otimes I_m) \\
&\times (-(d_x + c_x\frac{h}{T}\mu^{1/h})((\mathrm{L} \otimes I_m)x(t) + (\mathrm{L} \otimes I_m)H) \\
&- c_x\frac{h}{T}\frac{1}{T}\mu^{2/h}((\mathrm{L} \otimes I_m)x(t) + (\mathrm{L} \otimes I_m)H))] .
\end{aligned} \tag{42}
$$

From which we see that both u_y and $\dot{u}_y$ are continuous on $[t_0, t_1)$. Since $x(t)$ and $y(t)$ are continuous with respect to t according to (1) and (2). Therefore u_y is C^1 smooth with respect to t on $[t_0, t_1)$.

Step 5: The bipartite containment is kept and the control input u_y remains zero over $[t_1, \infty)$.

Selecting the Lyapunov function candidate identical to the one used in (31). We readily obtain:

$$
\begin{aligned}
&V_y \le -\frac{d\lambda_1(J)}{\lambda_{\max}(Q)} V_y \le 0, t \in [t_1, \infty) \\
&V_x \le -2 d_x \lambda_2(\mathrm{L}) V_x \le 0, t \in [t_1, \infty) .
\end{aligned} \tag{43}
$$

By noting that $x(t)$ and $y(t)$ are continuous at $t = t_1$, we then have $V_x(t)$ and $V_y(t)$ is continuous at $t = t_1$, and thus,

$$
\begin{aligned}
&V_y(t_1) = \lim_{t \to t_1^-} V_y(t) = 0 \\
&V_x(t_1) = \lim_{t \to t_1^-} V_x(t) = 0 ,
\end{aligned} \tag{44}
$$

both (43) and (44) yield

$$
\begin{aligned}
&0 \le V_y(t) \le V_y(t_1) = 0, t \in [t_1, \infty) \\
&0 \le V_x(t) \le V_x(t_1) = 0, t \in [t_1, \infty) .
\end{aligned} \tag{45}
$$

That is $V_y(t) \equiv 0$ and $V_x(t) \equiv 0$ on $[t_1, \infty)$. Thus $e_y(t) \equiv 0_{mn}$ and $e_x(t) \equiv 0_{mn}$, and then $u_y \equiv 0_{mn}$ on $[t_1, \infty)$. All of these imply that the bipartite containment is kept and the control input u_y remains zero over $[t_1, \infty)$ with the control law (9).

Step 6: We need to confirm the existence and continuity of u_y and $\dot{u}_y$ respect to t on $t = t_1$. $\lim_{t \to t_1^-} u_y(t) = u_y(t_1) = \lim_{t \to t_1^+} u_y(t)$, implying that u_y is exist and are continuous at $t = t_1$.

Now we prove that $\dot{u}_y$ is exist and are continuous at $t = t_1$. Upon using the fact that $\mu^{-1} \to 0$, $\mu^{1/h-1} \to 0$, $\mu^{2/h-1} \to 0$, as $t \to t_1^-$, we have $\lim_{t \to t_1^-} \dot{u}_y(t) = \dot{u}_y(t_1) = \lim_{t \to t_1^+} \dot{u}_y(t)$. Which means that u_y and $\dot{u}_y$ exist and are continuous with respect to t on $t = t_1$. We then concluded from the definition of continuousness and smoothness that u_y is C^1 smooth with respect to t over $[t_0, \infty)$.

4. Simulations

To evaluate the proposed prescribed-time formation-bipartite containment control method, we perform simulations using a two-layered MAS with eight agents. The systems comprise four leaders and four followers.

***Received**: 12 April 2024*
***Revised**: 24 April 2024*
***Accepted:** 6 May 2024*

DOI: https://doi.org/10.5281/zenodo.11123257

International Journal of Research (IJR)
e-ISSN: 2348-6848
p-ISSN: 2348-795X
Vol. 11 Issue 05
May 2024

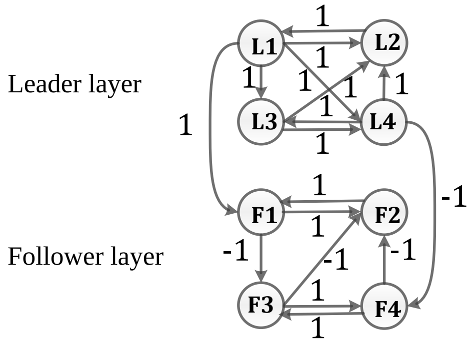

Fig 1.Communication topology（the number around each edge represents its weight）

According to the Fig 1 , the leadership communication topology among intelligent somite points is negative, and it only shows the cooperative relationship between them. On the other hand, the communication topology of the following points can be represented as a symbolic figure indicating both cooperative and competitive relationships between them. These relationships correspond to the adjacency matrix of points:

$$B = \begin{pmatrix} 0 & 1 & 0 & 0 \\ 1 & 0 & 1 & 1 \\ 1 & 0 & 0 & 1 \\ 1 & 0 & 1 & 0 \end{pmatrix}$$

$$A = \begin{pmatrix} 0 & 1 & 0 & 0 \\ 1 & 0 & -1 & -1 \\ -1 & 0 & 0 & 1 \\ 0 & 0 & 1 & 0 \end{pmatrix}$$

There is a restraining relationship between the agent 1 and agent 4 in the leader layer and the agent 1 and agent 4 in the follower layer, which is represented as the Fig 1. Follower agent layer can be divided into two groups:
$v_1^2 = \{1,2\}$ $v_2^2 = \{3,4\}$ .We have: $\eta^L = \{(1,2),(2,1),(3,1),(2,4),(3,4),(4,3),(2,3),(4,1)\}$, $\eta^F = \{(1,2),(2,1),(3,1),(2,4),(3,4),(4,3),(2,3)\}$, and it follows that $\eta^L \in \eta^F$, while η^L is not equal to η^F .

The initial states of the eight followers in x-axis, y-axis is set randomly. We select the design parameters as $T = 2.5$, $h = 2.5$, $c_x = 0.05$, $d_x = 2.5$, $c = 0.03$, $d = 15$.

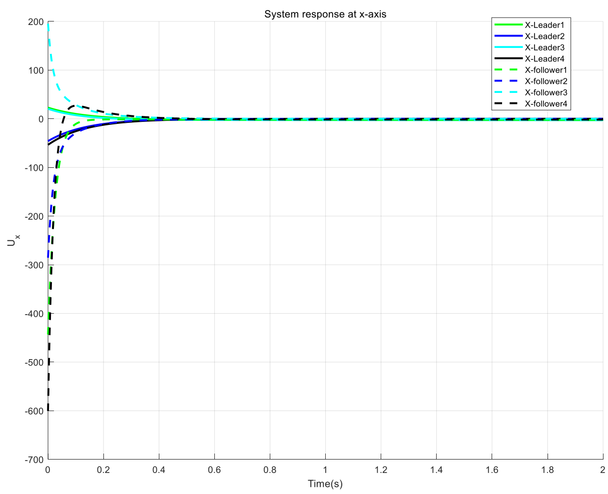

Fig 2. System response at x-axis.

***Received**: 12 April 2024*
***Revised**: 24 April 2024*
***Accepted:** 6 May 2024*

DOI: https://doi.org/10.5281/zenodo.11123257

e-ISSN: 2348-6848
p-ISSN: 2348-795X
Vol. 11 Issue 05
May 2024

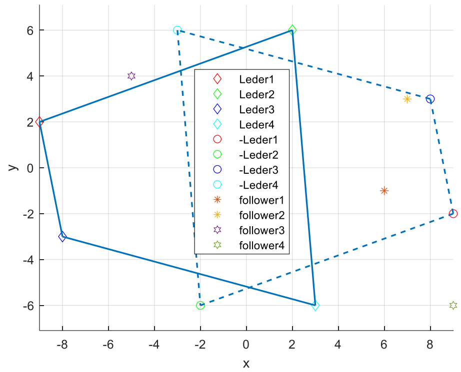

Fig 3. The trajectory of each agent at t=0s

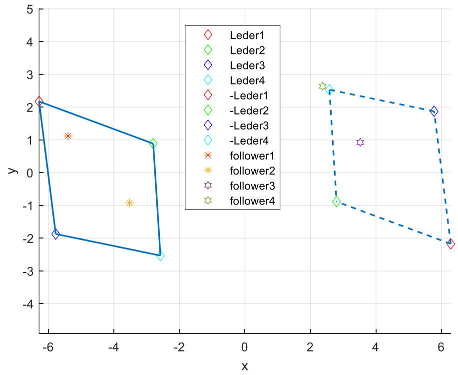

Fig 4. The trajectory of each agent at t=0.198s

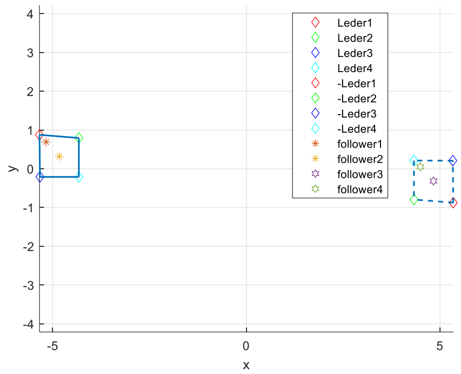

Fig 5. The trajectory of each agent at t=0.998s

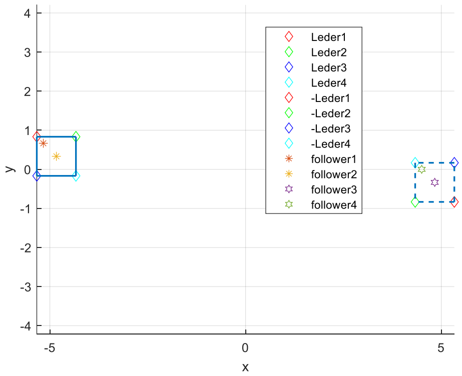

Fig 6. The trajectory of each agent at t=2s

The results of the formation bipartite containment control with the proposed control strategy are depicted in Fig 2-Fig 6, where Fig 2 is control input signal produced by (7) and (8), from the plot, we observe that the control input u_x and u_y of all the agents converge to zero within the specified finite time. Fig 3-Fig 6 is the drawing of agent in different time, within a specified time, the convex hull formed by leaders is indicated by solid lines. Follower 1 and 2 in the square formed by leaders, follower 3, and 4 into the square, which is formed by the symbolic opposite state of the leaders is marked by dotted lines. From Fig 6, it can be observed that the positions of the leaders maintain the desired regular square formation, and the positions of the followers remain within the convex hull formed by the leader positions in both the simulation and the experiment. Therefore, the specified time formation bipartite containment control is achieved.

5. Conclusion

This paper has investigated the formation bipartite containment of two-layered MASs. We presented a new prescribed-time distributed control method for the finite time control of two-layered MASs based on a time-varying feedback gain. The resultant control was able to achieve formation bipartite containment within a finite time that can be uniformly predetermined without relying on initial conditions or other design parameters. Furthermore, the control was distributed and C^1 smooth everywhere. The simulation and experimental results were presented to demonstrate the effectiveness of the obtained results. In the future, we planned to extend these results to two-layered MASs that were vulnerable to attacks.

References

[1] Geng H, Wu H, Miao J, et al. Consensus of heterogeneous multi-agent systems under directed topology[J]. IEEE Access, 2022, 10: 5936-5943.

[2] Xu C, Xu H, Guan Z H, et al. Observer-based dynamic event-triggered semiglobal bipartite consensus of linear multi-agent systems with input saturation[J]. IEEE Transactions on Cybernetics, 2022.

[3] Long J, Wang W, Wen C, et al. Output feedback based adaptive consensus tracking for uncertain

Received: *12 April 2024*
Revised: *24 April 2024*
Accepted: *6 May 2024*

DOI: https://doi.org/10.5281/zenodo.11123257

heterogeneous multi-agent systems with event-triggered communication[J]. Automatica, 2022, 136: 110049.
[4] Dong X, Hua Y, Zhou Y, et al. Theory and experiment on formation-containment control of multiple multirotor unmanned aerial vehicle systems[J]. IEEE Transactions on Automation Science and Engineering, 2018, 16(1): 229-240.Shan Q, Teng F, Li T, et al.
[5] Santiaguillo-Salinas, Jesús, and Eduardo Aranda-Bricaire. "Containment problem with time-varying formation and collision avoidance for multiagent systems." International Journal of Advanced Robotic Systems 14.3 (2017): 1729881417703929.
[6] Gao, Zhiyun, et al. "Time-varying output formation-containment control for homogeneous/heterogeneous descriptor fractional-order multi-agent systems." Information Sciences 567 (2021): 146-166.
[7] Jiang, Wei, et al. "Fully distributed formation-containment control of heterogeneous linear multiagent systems." IEEE Transactions on Automatic Control 64.9 (2018): 3889-3896.
[8] Zheng, Baojie, and Xiaowu Mu. "Formation-containment control of second-order multi-agent systems with only sampled position data." International Journal of Systems Science 47.15 (2016): 3609-3618.
[9] Wang, Yujuan, Yongduan Song, and Miroslav Krstic. "Collectively rotating formation and containment deployment of multiagent systems: A polar coordinate-based finite time approach." IEEE transactions on cybernetics 47.8 (2016): 2161-2172.
[10] Dong, Xiwang, et al. "Formation-containment analysis and design for high-order linear time-invariant swarm systems." International Journal of Robust and Nonlinear Control 25.17 (2015): 3439-3456.
[11] Xu Y, Qu Y, Luo D, et al. Distributed fixed-time time-varying formation-containment control for networked underactuated quadrotor UAVs with unknown disturbances[J]. Aerospace Science and Technology, 2022, 130: 107909.
[12] Duan, Jie, et al. "Fixed-time time-varying output formation–containment control of heterogeneous general multi-agent systems." ISA transactions 137 (2023): 210-221.
[13] Altafini C. Consensus problems on networks with antagonistic interactions[J]. IEEE transactions on automatic control, 2012, 58(4): 935-946.
[14] Meng D. Bipartite containment tracking of signed networks[J]. Automatica, 2017, 79: 282-289.
[15] Wang L, Han T, Zhan X S, et al. Bipartite containment for linear multi-agent systems subject to unknown exogenous disturbances[J]. Asian Journal of Control, 2022, 24(4): 1836-1845.
[16] Liu Y, Zhang H, Shi Z, et al. Neural-network-based finite-time bipartite containment control for fractional-order multi-agent systems[J]. IEEE Transactions on Neural Networks and Learning Systems, 2022.
[17] Liu Z, Zhan X, Han T, et al. Distributed adaptive finite-time bipartite containment control of linear multi-agent systems[J]. IEEE Transactions on Circuits and Systems II: Express Briefs, 2022, 69(11): 4354-4358.
[18] Wen G, Yu W, Zhao Y, et al. Node-to-node consensus of networked agents with general linear node dynamics[C]//2013 IEEE International Conference on Cyber Technology in Automation, Control and Intelligent Systems. IEEE, 2013: 24-29.
[19] WANG Yunyan, HU Aihua. Consensus of two-layer multi-agent systems subjected to cyber-attack[J]. Journal of Computer Applications, 2021, 41(5): 1399-1405.
[20] Wen G, Wang P, Huang T, et al. Distributed consensus of layered multi-agent systems subject to attacks on edges[J]. IEEE Transactions on Circuits and Systems I: Regular Papers, 2020, 67(9): 3152-3162.
[21] Wang L, Liu X, Cao J, et al. Fixed-time containment control for nonlinear multi-agent systems with external disturbances[J]. IEEE Transactions on Circuits and Systems II: Express Briefs, 2021, 69(2): 459-463.
[22] Guo X, Ma H, Liang H, et al. Command-filter-based fixed-time bipartite containment control for a class of stochastic multiagent systems[J]. IEEE Transactions on Systems, Man, and Cybernetics: Systems, 2021, 52(6): 3519-3529.
[23] Duan, Jie, et al. "Fixed-time time-varying output formation–containment control of heterogeneous general multi-agent systems." ISA transactions 137 (2023): 210-221.
[24] Wang L, Liu X, Cao J, et al. Fixed-time containment control for nonlinear multi-agent systems with external disturbances[J]. IEEE Transactions on Circuits and Systems II: Express Briefs, 2021, 69(2): 459-463.
[25] Wang Y, Song Y, Hill D J, et al. Prescribed-time consensus and containment control of networked multiagent systems[J]. IEEE transactions on cybernetics, 2018, 49(4): 1138-1147.
[26] Cartwright D, Harary F. Structural balance: a generalization of Heider's theory[J]. Psychological review, 1956, 63(5): 277.
[27] Han T, Chi M, Guan Z H, et al. Distributed three-dimensional formation containment control of multiple unmanned aerial vehicle systems[J]. Asian Journal of Control, 2017, 19(3): 1103-1113.

***Received**: 12 April 2024*
***Revised**: 24 April 2024*
***Accepted:** 6 May 2024*

 DOI: https://doi.org/10.5281/zenodo.11123257